# Spatially Resolved Transcriptomic Profiling Highlights Mechanisms Underlying Immune Activation in MSI Colorectal Tumors


**Daniel G. Camblor**[1,2], **Belén Martínez-Castedo**[1,2], **Francisco Gimeno-Valiente**[1], **Jorge Martín-Arana**[1,2], **Blanca García-Micó**[1,2], **Francisco Martínez-Picó**[1], **Alejandro Gimera**[1], **Diego González**[1], **Brenda Palomar de Lucas**[1], **Carolina Martínez-Ciarpaglini**[1,2], **Marisol Huerta**[1], **Susana Roselló**[1,2], **Desamparados Roda**[1,2], **Andrés Cervantes**[1,2], **Noelia Tarazona**[1,2]

[1] INCLIVA Biomedical Research Institute, Valencia, Spain
[2] Instituto de Salud Carlos III, CIBERONC, Madrid, Spain


## Background

**Microsatellite instability (MSI) colorectal cancers (CRC)** show better prognosis and immunotherapy response due to immune-infiltrated microenvironments, unlike most **microsatellite stable (MSS) tumors**.

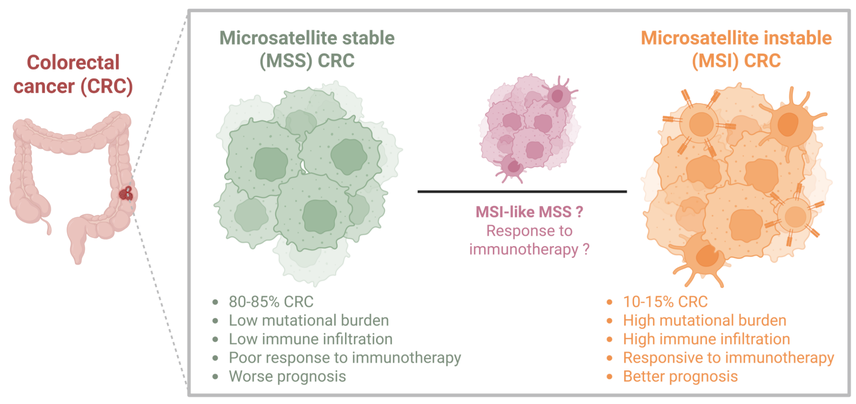


Understanding **MSI's** spatial immune drivers may improve **MSS** outcomes. Spatial transcriptomics offers a powerful approach to tackle this challenge.

## Methodology

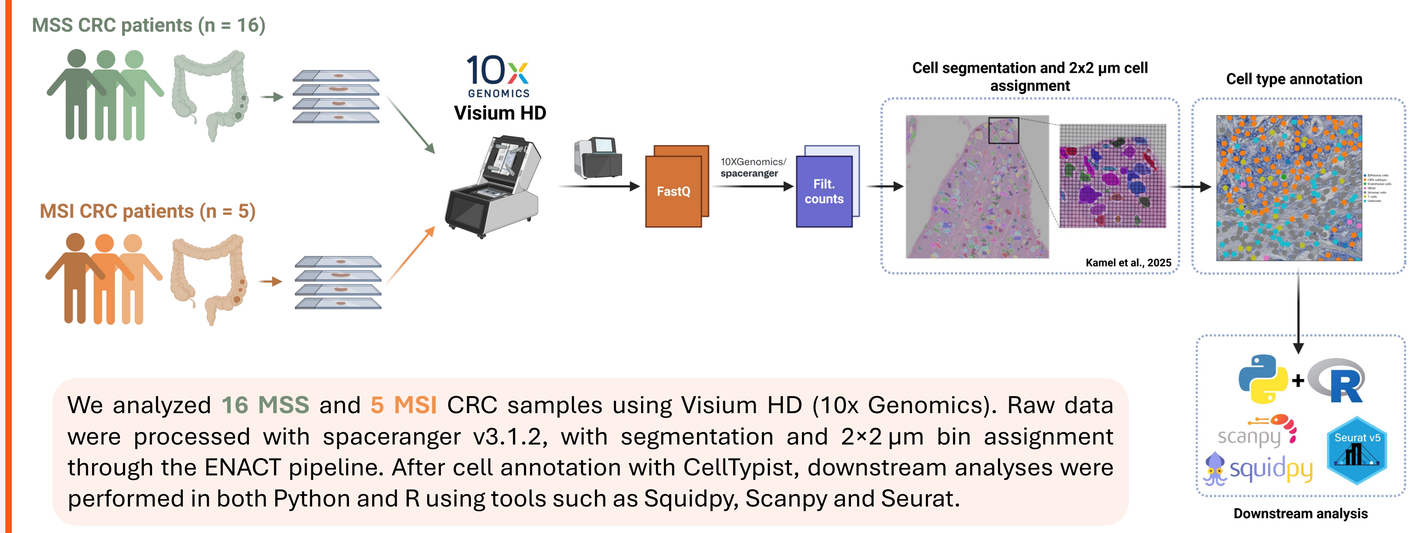


We analyzed **16 MSS** and **5 MSI** CRC samples using Visium HD (10x Genomics). Raw data were processed with spaceranger v3.1.2, with segmentation and 2×2 µm bin assignment through the ENACT pipeline. After cell annotation with CellTypist, downstream analyses were performed in both Python and R using tools such as Squidpy, Scanpy and Seurat.

## Results

We selected tumor cells in **MSS** and **MSI** samples (**Figure 1**), aggregated counts to pseudo-bulk and performed differential expression analysis. We found considerable variation between tumor cells of both types of CRC, identifying 989 differentially expressed genes with $|\log_2 FC| > 2$ (**Figure 2**).

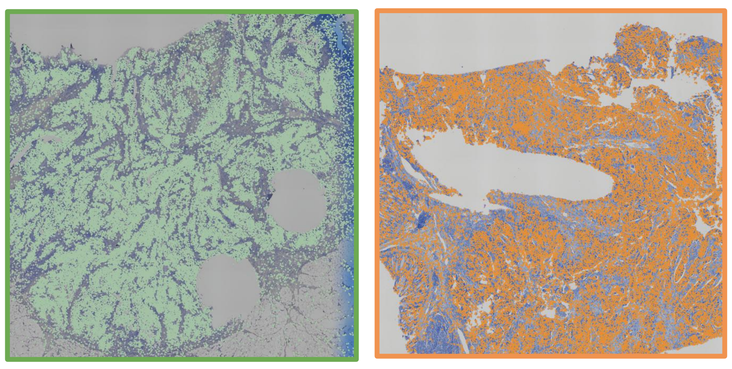

**Figure 1**. Selection of tumor cells in an **MSS** and an **MSI** sample.

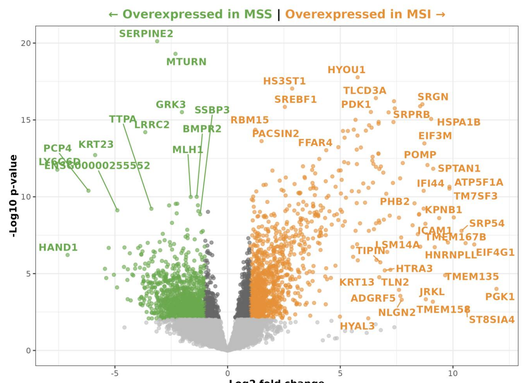


**Figure 2**. Differential expression analysis for **MSS** vs. **MSI** tumor cells.

While **MSI tumor cells** exhibited less Wnt and PPAR signaling activity (**Figure 3**), they in turn increased antigen processing and presentation, proliferation (cell cycle, DNA replication) and immune-related pathways (**Figure 4**).

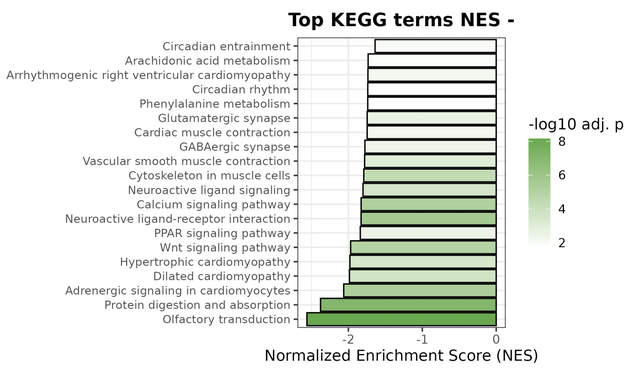


**Figure 3**. Top KEGG terms with negative (**MSS**) enrichment.

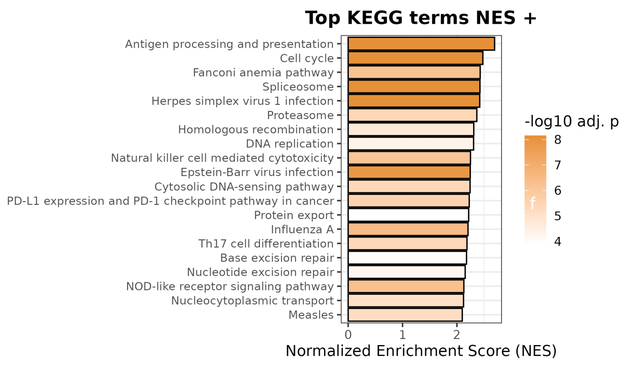


**Figure 4**. Top KEGG terms with positive (**MSI**) enrichment.

**MSI tumors** showed distinct cell composition profiles (**Figure 5**). Remarkably, they had more CMS1-like cells (tumor cells characterized by high mutational burden) and showed elevated immune infiltration, particularly of NK cells (**Figure 6**).

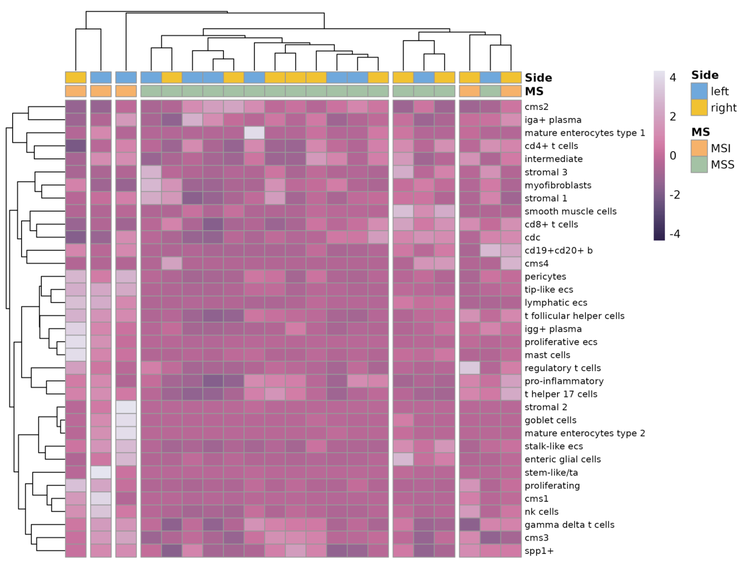


**Figure 5**. Heatmap showing the cell composition (%) in each sample. Some **MSS** samples tend to cluster near **MSI** samples.

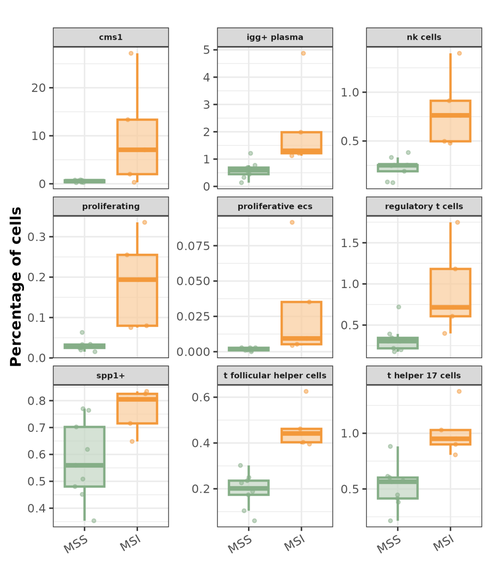


**Figure 6**. Cell types with significant (Wilcoxon $p < 0.05$) variation between **MSS** and **MSI** samples.

**MSI tumors** showed more prominent and structured immune infiltrates than **MSS tumors** (**Figure 7**), albeit with some exceptions. NK cell infiltrates were particularly involved (**Figure 8**).

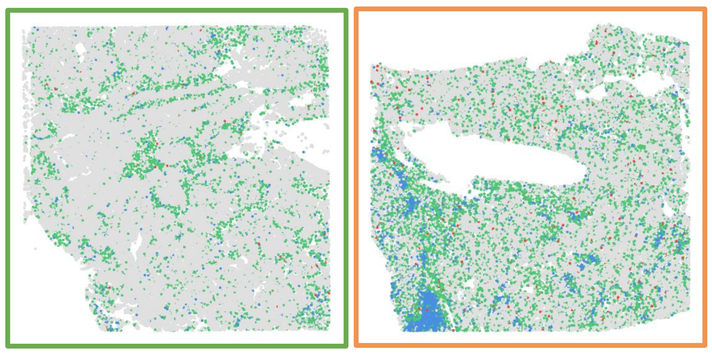

**Figure 7**. Immune infiltrates in **MSS** vs. **MSI** tumors. In green, T cells. In blue, B and plasma cells. In red, NK cells.

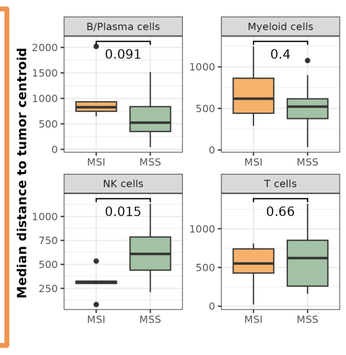


**Figure 8.** Immune cell distance to tumor core.

Spatially resolved pathway analysis using **MSI-specific signatures** like antigen processing and presentation (**Figure 9**) and cell cycle (**Figure 10**) allowed to better distinguish **MSS** and **MSI** tumors. Interestingly, some **MSS** tumors displayed intermediate features that put them closer to **MSI**.

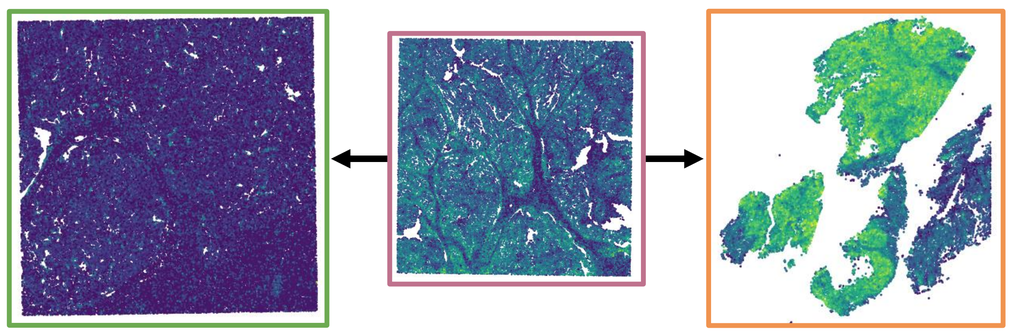

**Figure 9.** Antigen processing and presentation pathway (KEGG) scores in **MSS (left)** and **MSI (right)** samples. Some **MSS samples (center)** exhibit intermediate scoring.

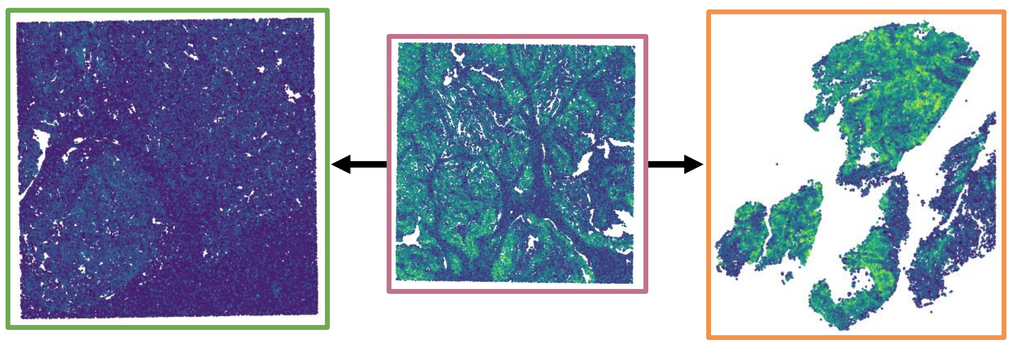

**Figure 10.** Cell cycle pathway (KEGG) scores in **MSS (left)** and **MSI (right)** samples. **Some MSS samples (center)** exhibit intermediate scoring.

Ligand-receptor inference revealed **MSI-** and **MSS-**specific ligand receptor interactions (**Figure 11**, **Figure 12**, respectively). **MSI tumors** mostly showed immune-activating interactions (e.g., TNF), while **MSS tumors** generally showed immune-repressing interactions (e.g., TGFB1).

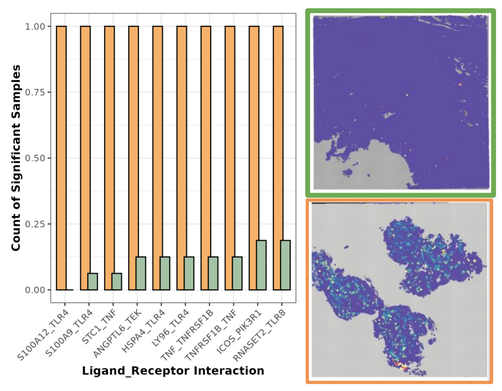


**Figure 11.** Top **MSI-specific** significant ligand-receptor interactions.

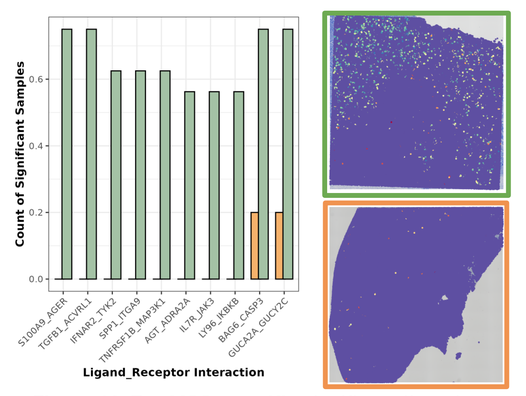


**Figure 12.** Top **MSS-specific** significant ligand-receptor interactions.

## Conclusions

**Spatial transcriptomics emerges as a technique of enormous utility to reveal actionable, spatially organized mechanisms of immune activation in CRC.**

**Although MSS and MSI CRC exhibit clear spatial differences, some MSS may have MSI-like features.**

**Exploiting our knowledge on MSS- and MSI-specific ligand-receptor interactions may lead to immunotherapy response in some MSS patients.**


@dgcamblor

dgonzalez@incliva.es



INCLIVA | VLC Biomedical Research Institute
Hospital Clínic Universitari de València
ciber | ONC
asociación española contra el cáncer en Valencia
X Bioinformatics Student Symposium
ISCB SC RSG-Spain